Am J Transl Res 2019;11(9):5390-5403
www.ajtr.org /ISSN:1943-8141/AJTR0097773

Original Article

Surface modification of decellularized trachea matrix with collagen and laser micropore technique to promote cartilage regeneration

Yong Xu[1*], Yaqiang Li[3*], Yanqun Liu[4*], Hao Li[4], Zihao Jia[4], Yao Tang[5], Gening Jiang[1], Xue Zhang[2], Liang Duan[1]

[1]Department of Thoracic Surgery, Shanghai Pulmonary Hospital, Tongji University School of Medicine, Shanghai, P. R. China; [2]Department of Dermatology, Xinhua Hospital, Shanghai Jiao Tong University School of Medicine, Shanghai, P. R. China; [3]Department of Orthopaedic Surgery, Shanghai 9th People's Hospital, Shanghai Jiao Tong University School of Medicine, Shanghai, P. R. China; [4]Research Institute of Plastic Surgery, Weifang Medical College, Weifang, Shandong, P. R. China; [5]Department of Hematology, The Second Affiliated Hospital of Nanchang University, Nanchang, Jiangxi, P. R. China. [*]Equal contributors.

Received May 16, 2019; Accepted August 16, 2019; Epub September 15, 2019; Published September 30, 2019

Abstract: The repair of long-segment tracheal defects remains a significant clinical challenge, to which, optimal biologically functioning tracheal alternatives may serve as a solution. Tissue-engineered trachea, regenerated from a decellularized trachea matrix using the laser micropore technique (LDTM), demonstrates the possibility of developing optimal tracheal substitutes, which retain the original tubular shape and adequate cartilage regeneration ability of trachea. However, the strict requirement with respect to the implantation cell density restricts the clinical translation of the LDTM, which has a low cell adherence rate. To overcome this problem, we propose a novel strategy involving collagen to modify the LDTM surface in order to enhance cell retention efficiency and promote homogeneous tracheal cartilage regeneration. The current results show that the modified LDTM significantly improves cell-seeding efficiency; moreover, it achieved stable cell retention and homogenous cell distribution. Additionally, at a relatively low implantation cell density (5.0×10^7 cells/mL, which is one-fourth of the cell-seeding density used in our previous study), homogeneous tubular cartilage was regenerated successfully both *in vitro* and *in vivo*. The cartilage had an exact tracheal shape, sufficient mechanical strength, typical lacuna structure, and cartilage-specific extracellular matrix deposition. Most importantly, the modified LDTM promoted chondrogenesis of the bone marrow-derived stem cells and the formation of homogeneous neocartilage *in vivo*. The current study has established a versatile and efficient cell-seeding strategy for the regeneration of multiple tissues. It also describes a technique for developing an optimal tracheal alternative for the repair and functional reconstruction of long-segment tracheal defects.

Keywords: Surface modification, cell-seeding efficiency, collagen, scaffold, cartilage

Introduction

Globally, the repair of long-segment tracheal defects remains a problem because of the scarcity of ideal substitutes [1, 2]. Among the potential replacements, a tissue-engineered trachea is considered to be the best candidate due to its favorable biocompatibility, low immunogenicity, high plasticity, and good biological activity [3-5]. Several artificially synthesized scaffolds, such as polylactic acid [6], polyglycolic acid [7], and polycaprolactone [8], are known to effectively repair the cartilage. However, their unfavorable biocompatibility, lack of bio-function, and the adverse effects of their degradation products limit their clinical application. Consequently, the lack of ideal scaffolds considerably restricts the clinical translation of tissue-engineered trachea [4].

The decellularized trachea matrix (DTM) is an ideal scaffold for tracheal cartilage regeneration due to its original tubular structure, natural cartilage matrix components, and excellent biocompatibility [9-11]. However, the dense cartilage matrix impedes the migration of cells into the DTM and leads to inadequate cartilage regeneration [12]. To overcome these prob-

lems, the laser micropore technique (LMT) described previously, was used to fabricate an LMT-treated DTM (LDTM); this procedure makes the trachea sample porous in order to facilitate decellularized treatment and cell ingrowth [13, 14]. Nevertheless, the large pore diameter (approximately 800 μm) and the arched and smooth surface of the LDTM, makes it considerably difficult for cells to attach and distribute evenly throughout the LDTM, especially on its micropores. Therefore, for homogenous tubular cartilage regeneration, an extremely high cell-seeding density (up to 2.0×10^8 cells/mL) was used in our previous study to enhance the viscosity of cell suspension; we achieved a better cell attachment and uniform distribution in the LDTM [13]. The requirement of high cell numbers considerably restricts the clinical translation of tissue-engineered trachea based on the LDTM due to the lack of an adequate cell source.

For overcoming the above-stated problems, it is necessary to establish an effective method to improve cell-seeding efficiency in order to achieve homogeneous cell distribution throughout the LDTM (as well as on the micropores and the LDTM surfaces). Type II collagen is currently the most widely used scaffold in clinical applications for cartilage repair; such a cell carrier might fulfill all the above requirements. Type II collagen-matrix guides cell migration, defines cell shape [15], and improves the synthesis of extracellular matrix by chondrocytes [16]. Moreover, collagen-which is unique to the cartilage-increases chondrogenesis in bone marrow-derived stem cells (BMSCs) [17, 18]. Therefore, collagen may be an ideal cell carrier for modifying the LDTM, enhancing cell-seeding efficiency, and for achieving a homogenous cell distribution.

The construction of tissue-engineered trachea involves paying considerable attention not only to the ideal scaffold but also to the appropriate cells that need to be seeded. Donor site morbidity, a limited quantity of chondrocytes, and dedifferentiation of chondrocytes into fibroblasts suggest that autologous chondrocytes are not an ideal cell source [19, 20]. BMSCs are attractive alternatives for tracheal cartilage repair because they are highly chondrogenic and can be expanded; moreover, donor site morbidity that is caused as a result of bone marrow aspiration is limited. A collagen-modified LDTM in combination with BMSCs, may serve as an ideal scaffold for construction of tissue-engineered trachea, because such a system would not only have an ability to induce cartilage repair, but would also provide a natural cartilage microenvironment [21-25].

Accordingly, the present study was conducted with the following objectives: 1) to test whether the collagen-modified LDTM has a higher adherence rate and can achieve even cell distribution as compared to the unmodified LDTM; 2) to verify that the chondrocyte-modified LDTM construct supports stable homogenous tubular tracheal cartilage regeneration with a relatively low cell concentration (specifically 5.0×10^7 cells/mL, which is only a quarter of the cell-seeding density used in a previous study) *in vitro* and *in vivo* [13]; 3) to test the hypothesis that the collagen-modified LDTM promotes chondrogenesis with BMSCs and forms homogenous tubular neocartilage *in vivo*.

Materials and methods

Experimental animals

The Shanghai Pulmonary Hospital Ethics Committee approved this project. Two-month-old New Zealand white rabbits with an average weight of 3.0 kg, were purchased from the Shanghai Jiagan Breeding Factory, Shanghai, China. Balb/c nude mice (lack of a thymus gland) were obtained from the Shanghai Institute of Materia Medica, Chinese Academy of Sciences, Shanghai, China.

Preparation of collagen-modified LDTM scaffold

The LDTM was prepared using previously established protocols [13, 14]; LDTM was cut into 1 cm long sections and inserted in a 1 cm long silicone tube (8.5 cm internal diameter), following which type II collagen solution (Sigma; 10 mg/mL in 0.1-M acetic acid) was injected into the gap between each silicone tube and the LDTM. The whole complex was frozen at -20°C for 24 h and was lyophilized until it was dry. The lyophilized scaffolds were treated with a carbodiimide solution (48 mM EDC and 6 mM NHS in 50-mM MES buffer; pH = 5.5) at -4°C for 24 h. The collagen-LDTM scaffold was rinsed with deionized water to remove the unreacted EDC

and NHS, and was lyophilized again. The collagen-LDTM scaffold was referred to as the modified group, whereas the pure LDTM scaffold was referred to as the control group; this is discussed in the next section.

Cell sourcing and culture

Auricular chondrocyte sourcing and culture: The auricular cartilage samples harvested from the New Zealand white rabbits were minced into approximately 1.0-mm^3 pieces and were digested for 8 h with 0.15% type II collagenase (Gibco) in Dulbecco's Modified Eagle Medium (DMEM, Gibco) at 37°C. Isolated chondrocytes were cultured in DMEM supplemented with 10% fetal bovine serum (FBS, Gibco) and 1% penicillin-streptomycin at 37°C under an atmosphere containing 5% CO_2. The cells at passage two (P2) were used for *in vitro* and *in vivo* cartilage evaluations.

BMSCs sourcing and culture: Following intravenous anesthesia with 5% sodium pentobarbital (0.5 mL/kg), 5 mL of bone marrow aspirate was harvested from the iliac crests of the New Zealand white rabbits, and was transferred into a 50-mL heparinized centrifuge tube. The BMSCs were isolated and expanded *in vitro*, as previously described [25]. The bone marrow was washed with DMEM, and centrifuged for 8 min at 200 *g*, following which the supernatant was removed. After that, the pellet was resuspended in the regular culture medium (DMEM supplemented with 10% FBS, 100 U/mL penicillin, and 100 U/mL streptomycin) and seeded in culture dishes. The sample was cultured for five days without changing the media to allow cells to get attached to the culture dishes; nonadherent cells were removed by media change. Subsequently, media changes were performed every three days. When cells were more than 80% confluent, they were digested with 0.25% trypsin plus 0.02% EDTA (Invitrogen) and subcultured at a density of 1.0×10^4 cells/cm^2 in a new plate. The cells at passage two (P2) were used for cartilage construction.

Cell distribution and proliferation of cell-scaffold constructs

Adherence rate: The chondrocytes at the second passage were seeded evenly onto the surface of the modified LDTM and pure LDTM at a density of 1×10^5 cells/mL. After 24 h incubation, the cell-scaffold constructs were rinsed gently with phosphate-buffered saline (PBS) to remove dead cells. The rinsing solution and the remaining cells in the culture dish were collected; the cells were counted, and cell number was represented as N. The adherence rate of scaffolds was calculated based on the formula: (total cell number - N)/total cell number × 100% [14, 26].

Cell proliferation assay: Cell proliferation in the modified and control groups was determined using the cell proliferation assay. Viable cells were analyzed by a Cell Counting Kit-8 assay (CCK-8; Dojindo, Japan) following the manufacturer's instructions. The optical density was measured at 450 nm, and the mean value was derived from five wells [8].

Live and dead cell viability assay: The viability of chondrocytes in the samples was determined at days 1 and 3 using the Live and Dead Cell Viability Assay (Invitrogen, USA), and was examined using a confocal microscope (Nikon, A1RMP, Japan).

In vitro and in vivo culture of chondrocyte-modified LDTM

The 1.0-cm long, tubular modified LDTM and pure LDTM scaffolds were sterilized using ethylene oxide. Chondrocytes at P2 were harvested and resuspended at a density of 5.0×10^7 cells/mL; 1.0 mL cell suspension was loaded evenly onto the modified LDTM and pure LDTM scaffolds, and all constructs were incubated at 37°C for 4 h and cultured in DMEM containing 10% FBS at 37°C under 5% CO_2. The medium was changed every two days. After five days of *in vitro* culture, the constructs were continuously cultured for four weeks or were subcutaneously implanted into nude mice and propagated for six weeks.

Morphology of constructs by SEM

Scanning electron microscopy (SEM; JEOL-6380LV, JP) was employed to detect changes on the surface of samples at various stages, including those before cell seeding and five days *in vitro* cultured cell constructs in the modified and control groups. The samples were rinsed with PBS and fixed overnight in 0.05% glutaraldehyde at 4°C. After dehydration through a graded series of ethanol, the sam-

ples were critical-point dried and examined by the SEM.

Chondrogenesis of BMSCs-modified LDTM construct

P2 BMSCs were seeded evenly onto the surface of the modified LDTM and pure LDTM scaffolds at a density of 5.0×10^7 cells/mL. After incubation at 37°C for 4 h, the constructs were cultured in DMEM containing 10% FBS at 37°C under 5% CO_2. After maintenance in *in vitro* conditions for four weeks, the BMSCs-modified LDTM constructs were used for gene testing or were subcutaneously implanted into nude mice and propagated for 8 or 16 weeks.

Real-time polymerase chain reaction (RT-PCR)

After 1, 14, and 28 days of *in vitro* culture, the total RNA from the BMSC-collagen-LDTM constructs was extracted using the standard TRizol procedure (Invitrogen). The concentration and purity of the RNA were checked using a NanoDrop ND-2000 Spectrophotometer (Thermo Fisher, Wilmington, MA, USA). To ensure the purity of the RNA, only samples with a 260/280 nm absorbance ratio of >1.8 were analyzed. The mRNA was reverse-transcribed into cDNA using a ReverTra Ace kit (Toyobo, Osaka, Japan). Reactions were conducted at 95°C for 10 min, followed by 40 cycles at 95°C for 15 s, 58°C for 15 s, 72°C for 35 s, and finally 60°C for 1 min. The expressions of aggrecan, SOX9, and type II collagen genes were quantified using an RT-PCR on a LightCycler 480 system (Roche Applied Science, Indianapolis, IN, USA). The target genes were amplified using the following specific primers: aggrecan (XM_002723376.1, forward: 5'-GGAGGAGCAGGAGTTTGTCAA-3' and reverse: 5'-TGTCCATCCGACCAGCGAAA-3'); SOX9 (XM_002719499, forward: 5'-GCGGAGGAAGTCGGTGAAGAAT-3' and reverse: 5'-AAGATGGCGTTGGGCGAGAT-3'); collagen II (XM_002723438.1, forward: 5'-CACGCTCAAGTCCCTCAACA-3', and reverse: 5'-TCTATCCAGTAGTCACCGCTCT-3'). The housekeeping gene, glyceraldehyde-3-phosphate dehydrogenase (GAPDH), was used as a reference gene (NM_001082253.1, forward: 5'-CAAGAAGGTGGTGAAGCAGG-3' and reverse: 5'-CACTGTTGAAGTCGCAGGAG-3'). The mRNA levels of aggrecan, SOX9, and collagen II were normalized to the levels of GAPDH mRNA at the corresponding time points [27].

Histological analysis

Samples, including those cultured *in vitro* and *in vivo*, were fixed in 4% paraformaldehyde, embedded in paraffin, and sectioned. The sections were stained with hematoxylin and eosin and safranin-O to evaluate the structure and deposition of the cartilage extracellular matrix (ECM) in the engineered tissue. The expression of type II collagen was detected as previously described [13] to further verify the cartilage-specific phenotype.

Quantitative analysis

All samples from the various groups, including pure LDTM, native trachea cartilage, *in vivo*-engineered cartilage by chondrocytes, and BMSCs were cut into squares (0.5×0.5 cm^2). Quantitative analyses were performed as described below.

Mechanical tests

Tensile tests were performed using a biomechanical analyzer (Instron 5542 Canton, USA) along the longitudinal direction up to the rupture, as confirmed by the loss of load and the appearance of tears in the tissue. The specimens were clamped into the sample holders, and testing was initiated with a constant elongation rate of 1 mm/min at room temperature. The biomechanical analyzer recorded the load and elongation of the tissue in real-time. Maximum tensile forces were recorded for statistical analysis [13]. For the evaluation of radial properties, neocartilage specimens and native trachea specimens were placed on their sides between the compression plates. Complete radial compression of cylindrical constructs was performed at a strain rate of 1 mm/min. Radial compression was performed to a maximum deformation equaling 60% of the original diameter. The samples were subjected to a continuous planar unconfined strain rate of 1 mm/min until 80% of the maximal deformation was achieved; Young's modulus of the tested samples was calculated based on the slope of the stress-strain curve.

Wet weight and thickness

The samples from the various groups were weighed with an electronic balance, and their thickness was measured with a Vernier caliper.

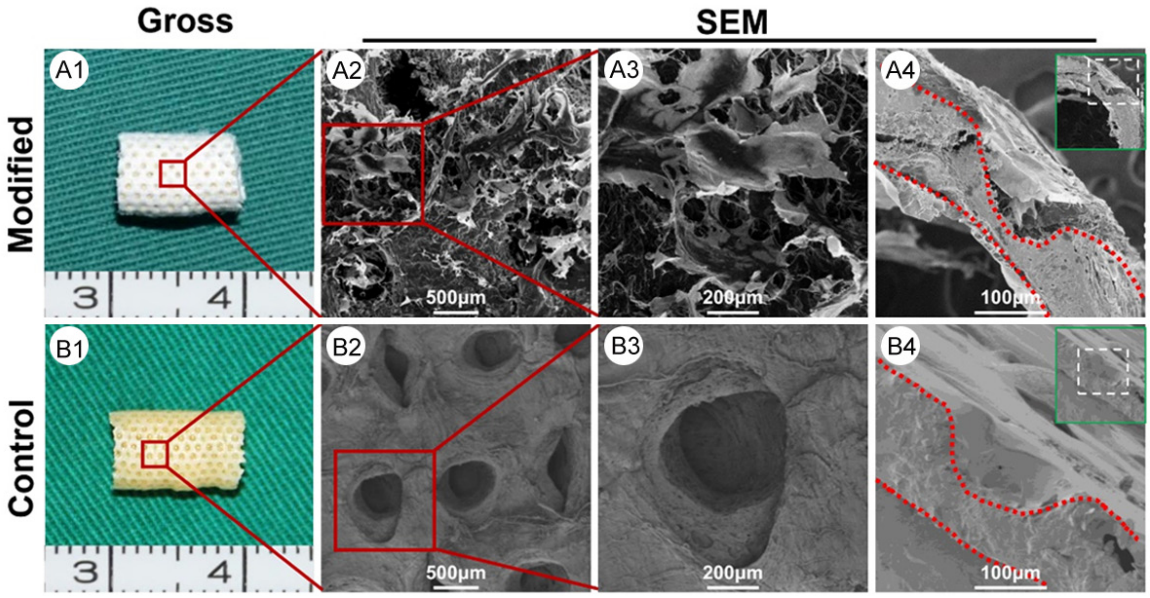

Figure 1. Surface topography of the modified and control groups. The gross and SEM views show evenly distributed porous collagen scaffold on all surfaces and the laser micropores of the LDTM in the modified (A1-A3), but not in the control group (B1-B3), thereby increasing the porous structure and expanding the surface for cell adhesion. Imaging of the transverse section (A4 and B4) by SEM confirmed these results. The red dotted lines indicate the borders of LDTM.

Differences in wet weight and thickness among the groups were analyzed by one-way analysis of variance.

Biochemical analyses

The specimens were digested using a papain solution (Sigma-Aldrich) at 65°C. The sulfated glycosaminoglycan (GAG) content was quantified by alcian blue method [22, 28]. The genomic DNA, after ethanol extraction and column adsorption, was recovered in the elution buffer. The DNA content was detected using a nucleic acid and protein quantitation detector (Nanodrop 2000); each sample was analyzed three times. The total collagen content in various groups was quantified by hydroxyproline assay. The samples were prepared by alkaline hydrolysis, and free hydroxyproline hydrolysates were assayed as described earlier [29].

Statistical analysis

All data were analyzed using GraphPad Prism 5.0, and presented as mean ± standard deviation with $n = 5$; Two-tailed Student's t-test was used to assess the statistical significance of results ($P<0.05$).

Results

Surface modification of LDTM

The topographies of the modified LDTM and pure LDTM scaffolds were evaluated initially based on gross and SEM observation. After even modification with collagen, the modified LDTM exhibited a porous structure both the surface as well as inside the laser micropores (**Figure 1A1-A3**); this was also confirmed by the transverse section image captured by SEM (**Figure 1A4**). In the group without collagen (control group), only laser micropores were observed, and the remaining surfaces were verified by gross and SEM observations (**Figure 1B1-B4**). The results indicated that the modified group had a more porous structure for cell seeding.

In vitro cell seeding

After cell seeding, the Live and Dead staining assay was used to analyze survival and proliferation of chondrocytes in both groups. Relatively homogeneous cell distribution was observed in the modified group (**Figure 2A1** and **2A2**), but not in the control group (**Figure 2B1** and **2B2**). Moreover, distinct cell loss

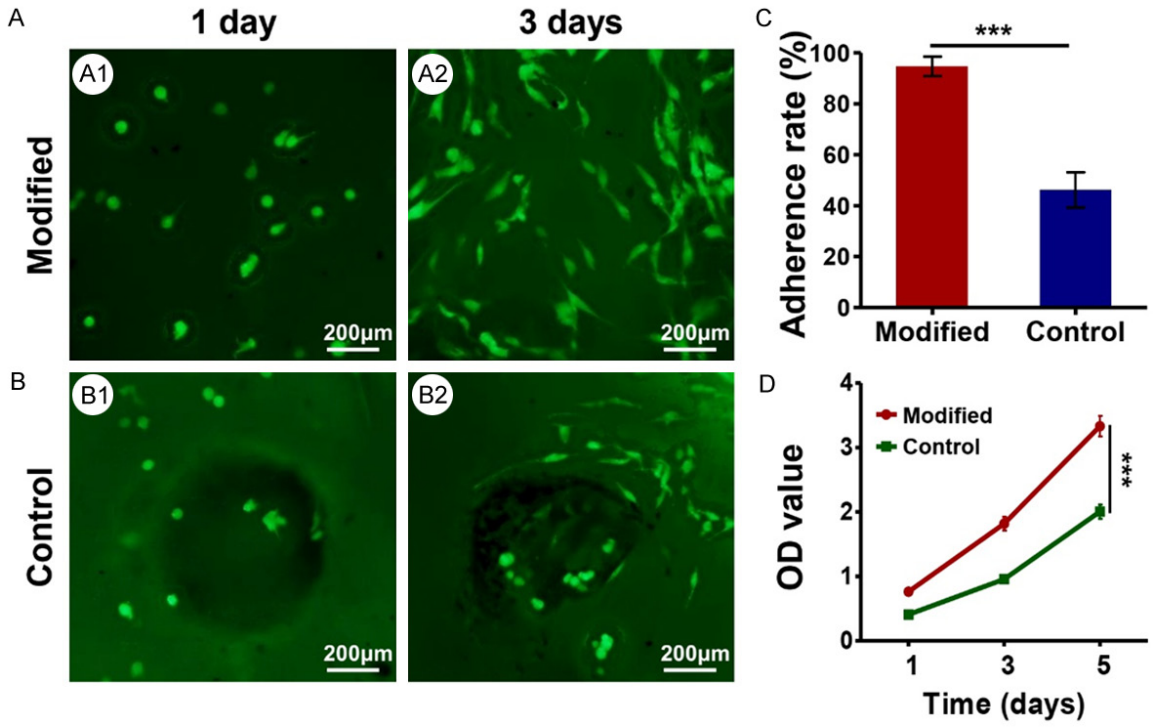

Figure 2. Distribution and proliferation of chondrocytes in the modified and control groups. The Live and Dead assay staining shows the survival and proliferation of chondrocytes in both groups (A, B); However, a relatively homogeneous cell distribution is observed only in the modified group (A1 and A2). Further, a less dense and nonhomogeneous cell distribution is seen in the control group (B1 and B2). Quantitative analyses show significantly higher adherence rate at 24 h (C), and DNA content, on 1, 3, and 5 days (D) in the modified group compared to the control group. ***: $P<0.001$.

inside the laser micropores was observed in the control group (**Figure 2B1** and **B2**). Quantitative analyses showed a significantly higher adherence rate (at 24 h) (**Figure 2C**) and cell proliferation on days 1, 3, and 5 (**Figure 2D**) in the modified group compared to the control group. These results showed a homogeneous cell distribution and improved cell adherence rate in the modified group; hence, it is expected to enhance cartilage regeneration significantly.

Cartilage regeneration in vitro and in vivo

Cartilage regeneration was evaluated first in *in vitro* studies. After *in vitro* culture for 5 days, chondrocytes produced abundant ECM to cover all micropores and the entire surface in the modified group (**Figure 3A1-A3**). In marked contrast, the nonhomogeneous ECM distribution and laser micropores can be observed distinctly in the control group (**Figure 3B1-B3**). After four weeks of *in vitro* culture, the samples in the modified group formed homogeneous tubular cartilage-like tissues, and the continuous neocartilage completely covered the surfaces and filled the micropores (**Figure 4A1**). Histology results showed that cells secrete abundant homogeneous ECM to cover both micropores and surfaces (**Figure 4A2**) as evidenced by the positive staining for GAG (**Figure 4A3**) and collagen II (**Figure 4A4**). In sharp contrast, a relatively thin irregularly shaped nonhomogeneous cartilage was observed in the control group (**Figure 4B1-B4**).

The feasibility of homogeneous cartilage regeneration *in vivo* was explored further. After 5 days of *in vitro* pre-culture and six weeks of subcutaneous implantation, the results were consistent with those obtained *in vitro* (including gross view and histological examination) (**Figure 5A1-A4** and **5B1-B4**). All quantitative evaluations of the *in vivo* engineered cartilage, including wet weight (**Figure 6A**), thickness (**Figure 6B**), DNA content (**Figure 6C**), GAG content (**Figure 6D**), total collagen (**Figure 6E**), breaking force (**Figure 6F**), compression force (**Figure 6G**), and Young's modulus (**Figure 6H**),

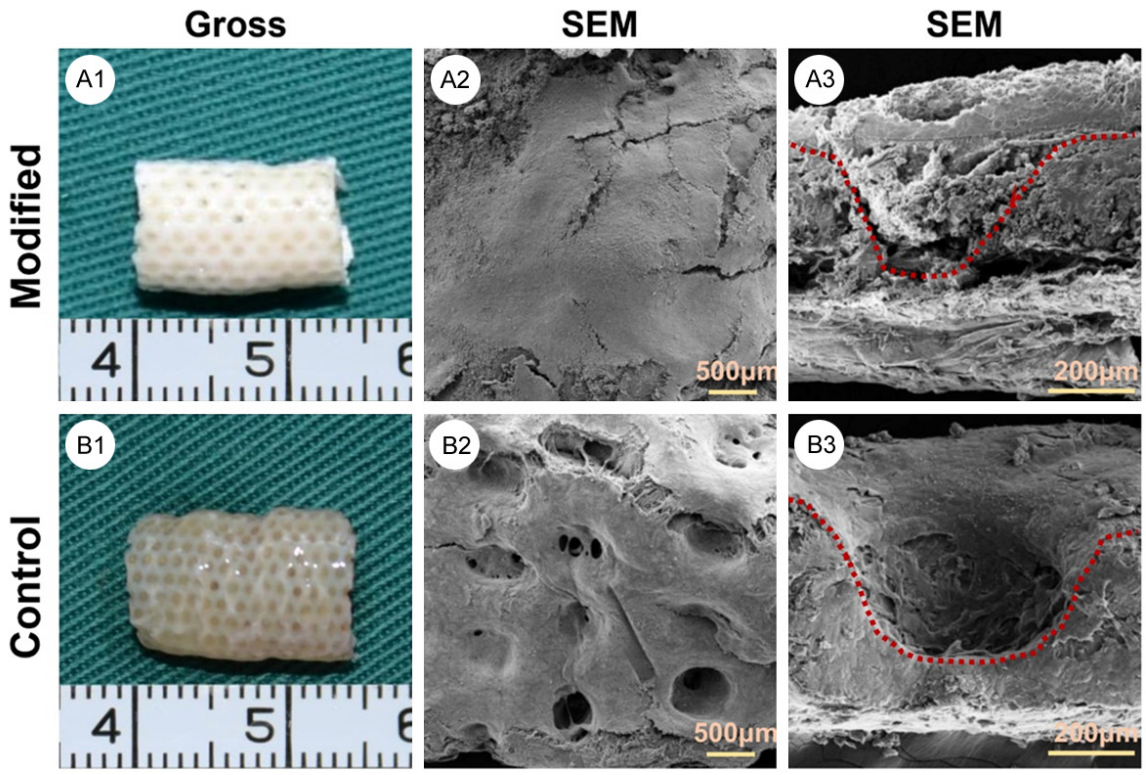

Figure 3. Cell-scaffold construct. After chondrocyte seeding and *in vitro* culture for 5 days, the chondrocytes produce abundant ECM to cover all micropores and entire surfaces in the modified group (A1-A3). Conversely, nonhomogeneous and less dense ECM distribution, and exposed laser micropores can be observed distinctly in the control group (B1-B3). SEM images of the transverse section also confirm the above conclusions (A3 and B3). The red dotted lines indicate the borders of LDTM.

were significantly higher in the modified group than those in the control groups (and the other groups). The above results indicated that the LDTM at a low cell-seeding concentration (5.0×10^7 cells/mL) failed to form satisfactory cartilage without surface modification.

Chondrogenesis using BMSC-modified LDTM construct

Cartilage regeneration using BMSCs as seeding cells is another important basis for predicting the feasibility of a future clinical application. After seeding the BMSCs onto the modified LDTM and culturing for 1, 14, and 28 days *in vitro*, the real-time gene expression results showed fold-increases in collagen II (**Figure 7A**), aggrecan (**Figure 7B**), and SOX9 (**Figure 7C**) expression. Moreover, after 8 and 16 weeks of *in vivo* culture, the samples formed elastic, homogeneous, ivory-white cartilage-like tissues that were comparable to the tissues formed by samples seeded with chondrocytes (**Figure 8**). Histologically, all samples exhibited the typical features of cartilage tissue, with abundant lacuna structures and cartilage-specific ECM deposition (**Figure 8A2-A4** and **8B2-B4**). Moreover, the neocartilage matured with an extended culture time of 8-16 weeks; characterized by a whiter appearance, more typical lacuna structures, and a thicker cartilage layer, which were confirmed by the quantitative analyses of the DNA, GAG, and total collagen content, and the values of breaking force, compression force, and Young's modulus (**Figure 9**). These results indicate that in combination with BMSCs, the modified LDTM is an ideal scaffold for chondrogenesis induction.

Discussion

To date, there is no clinically available tracheal substitute because many attempts to produce an autologous or synthetically safe and reproducible tracheal graft have failed; this undermines the future of long-segment tracheal

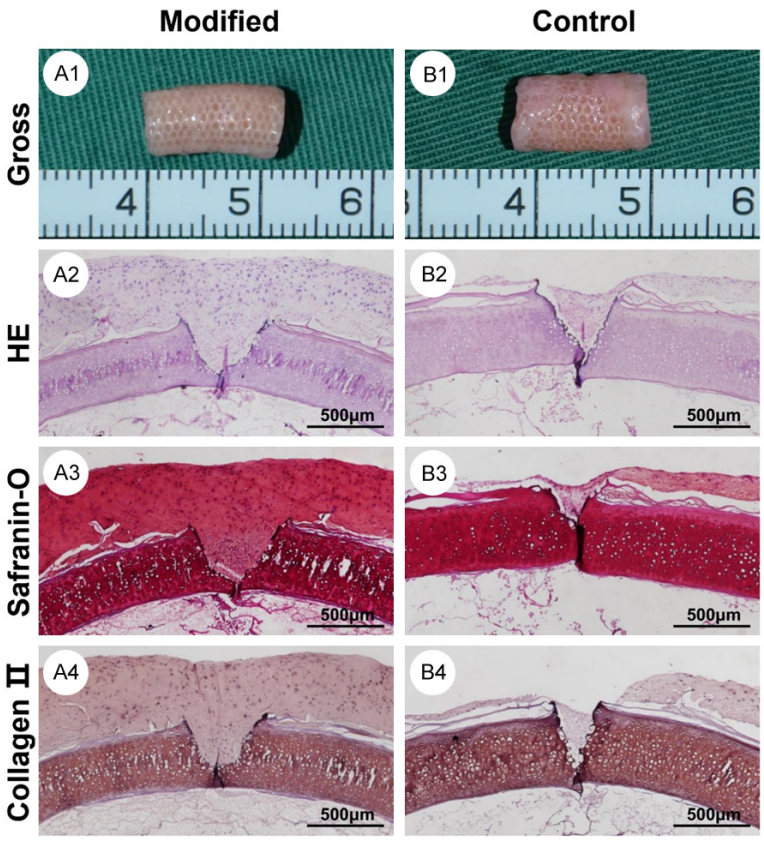

Figure 4. *In vitro* tracheal cartilage regeneration. The modified group forms homogeneous cartilage-like tissue (A1). Histologically, the cells secrete abundant homogeneous ECM to cover both micropores and surfaces (A2), which stained positive for glycosaminoglycan (GAG) (A3) and collagen II (A4). However, a relatively thin and nonhomogeneous engineered cartilage with an irregular shape is observed in the control group (B1-B4). The seeded cells are rabbit auricular chondrocytes.

replacement [30-32]. Tissue-engineered tracheal cartilage regeneration based on the LDTM demonstrates the possibility of developing an ideal tracheal substitute with a natural tubular shape, excellent cartilage regeneration ability, adequate mechanical properties, and ECM components that are similar to that of the native trachea [13, 14]. However, the rigid implantation cell density requirement substantially restricts the clinical translation of the LDTM, which has a low cell adherence rate [33]. The current study addresses this challenge by proposing the use of collagen as a substrate for increasing the cell retention ability of the LDTM to improve tracheal cartilage regeneration. The results showed that collagen-modified LDTM significantly enhanced the cell-seeding efficiency and achieved stable cell retention as well as homogenous cell distribution throughout the LDTM. Moreover, a satisfactory homogeneous tubular cartilage was regenerated successfully using the collagen-modified LDTM *in vitro* and *in vivo* with a relatively low cell-seeding density (5.0×10^7 cells/mL, which was only a quarter of the cell-seeding density that was used in our previous study [13]). Most importantly, the modified LDTM promoted the chondrogenesis of BMSCs and formed a homogeneous neocartilage *in vivo*. These results provide a feasible strategy for the long-segment tracheal cartilage regeneration and its clinical translation.

Although the results from our previous study showed an acceptable tubular cartilage regeneration based on the LDTM, the strict implantation cell density (2.0×10^8 cells/mL) requirement considerably restricts its clinical translation. A high implantation cell density is required for LDTM because it has a low cell adherence rate due to the presence of overlarge micropores, and because of its arched and smooth surface; evidently, these features are unfavorable for cell adhesion and retention. The trachea, as a unique tubular structure, poses a substantial challenge for cell adhesion and retention. The current study addressed this by modifying the LDTM with collagen to enhance the cell-seeding efficiency and to achieve homogeneous cell distribution. The results show the formation of a porous structure on the surface and inside the laser micropores of the modified LDTM. The porous collagen structure displayed excellent biocompatibility and provided a natural three-dimensional (3D) biomimetic microenvironment that supported chondrocyte survival, proliferation, ECM production, and cartilage regeneration. After seeding, the cells got firmly attached to the porous collagen structure and were distributed evenly on the

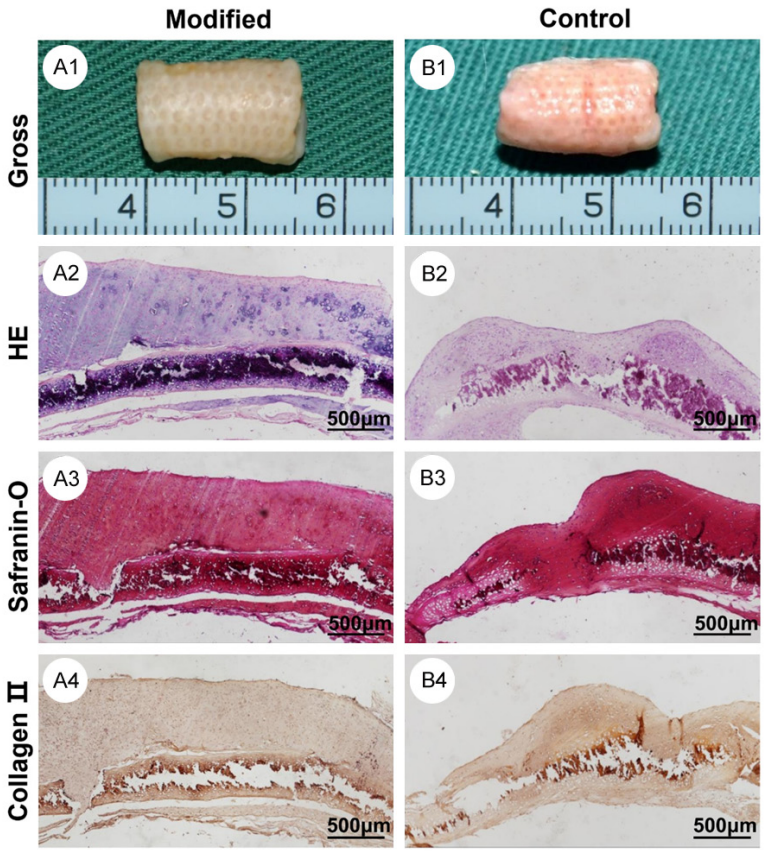

Figure 5. *In vivo* tracheal cartilage regeneration. Similar to the *in vitro* results, the modified group forms homogeneous cartilage-like tissues *in vivo* (A1). Histologically, cells secrete abundant homogeneous ECM to cover the micropores and surfaces (A2) which stain positive for GAG (A3) and collagen II (A4). In contrast, a relatively thin and nonhomogeneous engineered cartilage with an irregular shape is observed in the control group (B1-B4). The seeded cells are rabbit auricular chondrocytes.

surface and in the micropores; thus, collagen contributed significantly to considerably higher cell-seeding efficiency and DNA content in the modified group compared to the control group. These results collectively indicate the feasibility of using collagen as a carrier to improve cell seeding and distribution.

After addressing the challenges in cell seeding and distribution, the next crucial question is whether the homogeneous tracheal cartilage can be regenerated successfully using a relatively low cell-seeding concentration in the modified LDTM. This is important as it relates directly to the future clinical applicability of this method [34-36]. As expected, after 5 days or four weeks of *in vitro* culture, and six weeks of subcutaneous implantation in nude mice, the chondrocyte-modified LDTM constructs with an initial implantation cell density of 5.0×10^7 cells/mL, formed homogeneous cartilage-like tissues with a perfect trachea shape, adequate mechanical strength, and good elasticity. Histological examination further showed that the regenerated trachea cartilage possessed a chimeric structure composed of typical neocartilage and residual LDTM scaffold with acceptable interface integration. Furthermore, the neocartilage completely filled the micropores and covered the surfaces to sufficiently surround the residual LDTM scaffold. In contrast, the chondrocyte-LDTM constructs (control group) formed relatively thin and nonhomogeneous cartilage with an irregular shape and prominently visible micropores with inferior mechanical properties and reduced elasticity. These observations suggest that the chondrocyte-LDTM constructs failed to form a suitable cartilage without a cell carrier at a low chondrocyte concentration (5.0×10^7 cells/mL). Evidently, in the modified group, the adequate cartilage regeneration observed on using a relatively low implantation cell density was attributed to the high cell-seeding efficiency, excellent biocompatibility, low cytotoxicity, and a natural 3D biomimetic microenvironment provided by the collagen and the LDTM. Based on the current results, the quantitative indices, including wet weight, thickness, DNA content, GAG content, total collagen, breaking force, compression force, and Young's modulus, in the modified group were not only significantly higher than those in the control group, but were also even higher than those in the native tracheal tissue. Thus, implying that a lower cell-seeding concentration with collagen as a carrier might also regenerate adequate amount of tracheal cartilage; consequently, this finding has a higher clinical significance.

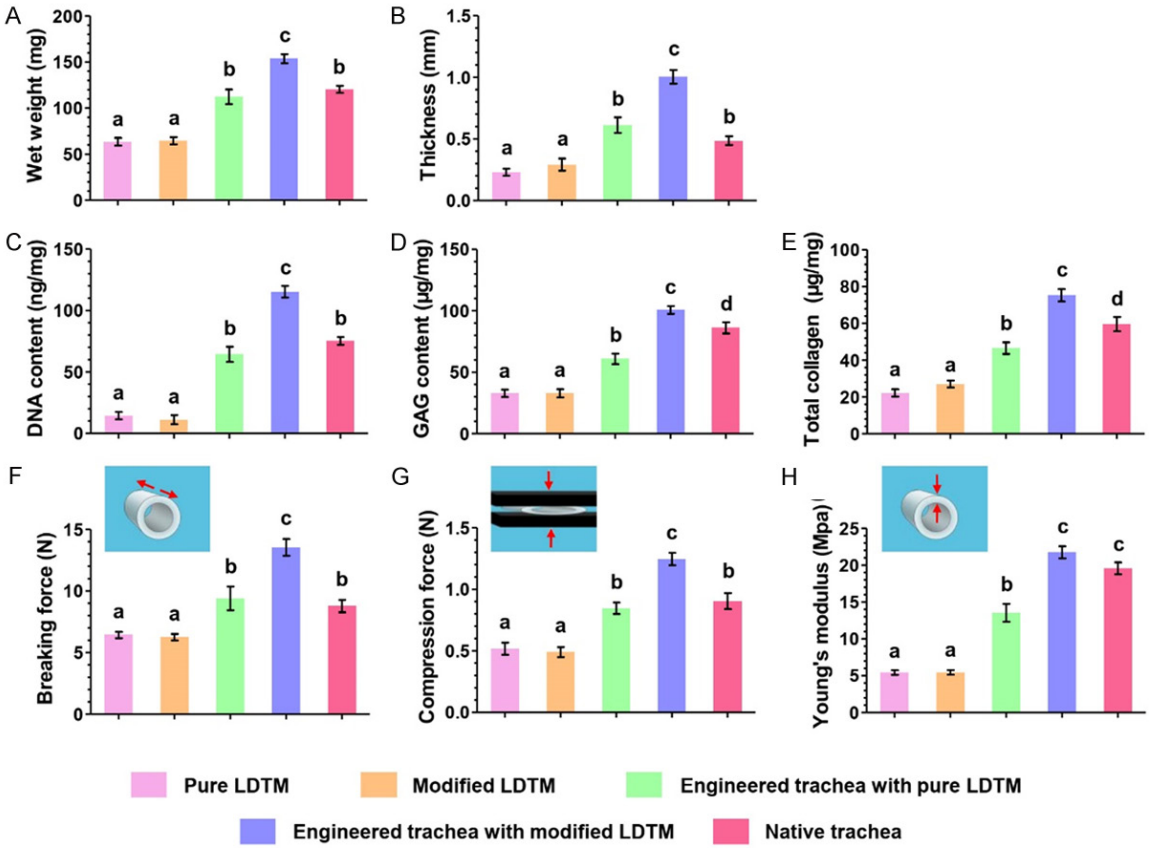

Figure 6. Quantitative evaluations of the engineered cartilage in nude mice. All quantitative indices, including wet weight (A), thickness (B), DNA content (C), GAG content (D), total collagen (E), breaking force (F), compression force (G), and Young's modulus (H), are significantly higher or comparable in the modified group than those in the other groups. The indices in the control group are evidently higher compared to those of the pure and modified LDTM scaffolds, but are lower than those of fresh native trachea. Letters in lowercase indicate significant differences among the groups (P<0.05). The red arrows indicate the direction of the force.

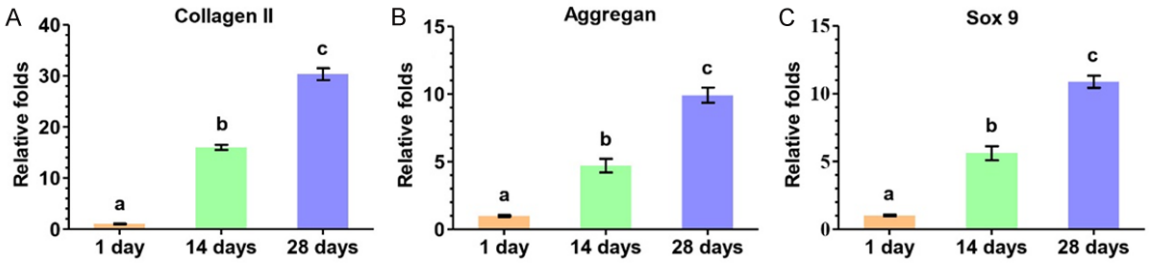

Figure 7. Gene expression levels in the background of chondrogenic induction using BMSCs *in vitro*. The real-time gene expression results from BMSC-modified LDTM construct *in vitro* on days 1, 14, and 28 show the fold-increases in collagen II (A), aggrecan (B), and SOX9 (C) gene expression, which indicate that BMSCs are gradually differentiating into cartilage. Lowercase letters indicate significant differences among groups (P<0.05).

Although the use of chondrocytes is prevalent in cartilage tissue engineering applications, the concerns associated with donor-site morbidity, cell dedifferentiation, and limited lifespan of chondrocytes have led to the use of BMSCs [37]. The BMSCs seem to be the right cell type for tissue-engineered cartilage regeneration because of their chondrogenic capacity, and their ease of isolation and expansion *in vitro* [38, 39]. The function of native trachea carti-

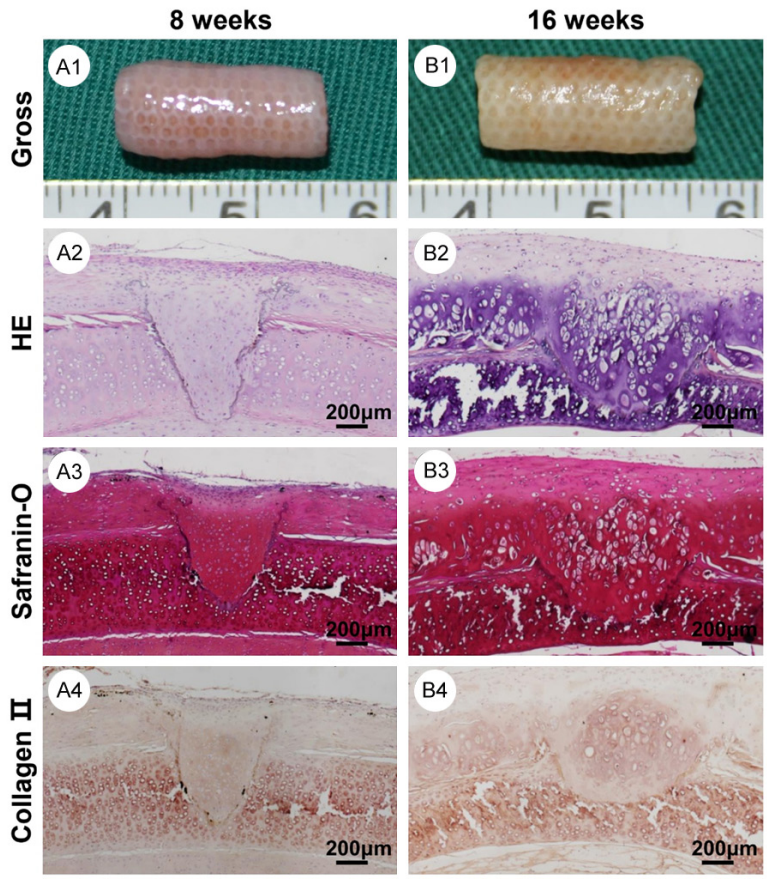

Figure 8. *In vivo* chondrogenesis using the BMSC-modified LDTM construct. After cell seeding, the BMSCs are evenly distributed on the modified LDTM which form homogeneous cartilage-like tissues that exhibit a partially mature cartilage appearance from 8 to 16 weeks (A1-A4 and B1-B4). Histologically, the engineered cartilage induced by the BMSCs is primarily formed at eight weeks with typical lacunae structures and cartilage-specific ECM deposition (A2-A4); it matures as a function of extended *in vivo* culture time as confirmed by larger lacuna structure and increased cartilage matrix secretion (B2-B4).

lage can be attributed to the presence of unique structural proteins that are a part of an organized extracellular network, which is composed mainly of type II collagen [40]. Collagen is a very promising material, which is used in a wide range of tissue engineering applications due to its excellent biocompatibility, biodegradability, and cell-binding properties [40, 41]. Moreover, type II collagen increases the chondrogenesis of BMSCs [17, 18]. The LDTM also provides a natural chondrogenesis microenvironment for BMSCs [42, 43]. As a result, the collagen-modified LDTM supports the chondrogenesis of BMSCs. The current study demonstrates that the collagen-modified LDTM is suitable for chondrogenic inducement with BMSCs and formation of homogeneous tubular cartilage during *in vitro* and *in vivo* culture; thus suggesting the feasibility of its future clinical application.

Conclusion

In summary, the collagen-modified LDTM scaffold is an effective strategy to achieve even cell distribution and successful homogeneous tubular cartilage regeneration with relatively low cell-seeding densities. In addition, our study showed that the collagen-modified LDTM could induce cartilage regeneration with the BMSCs. The current study has established a versatile, highly efficient cell-seeding strategy for various types of tissue regeneration. We also present a technique that yields an optimal tracheal substitute for the repair and functional reconstruction of long-segment tracheal defects. Nevertheless, the feasibility of using this system for *in situ* tracheal defect repair, epithelialization, and vascularization, needs to be investigated in the future.

Acknowledgements

This work was supported by the National Natural Science Foundation of China (81570089, 81270070), Natural Science Foundation of Shanghai (19ZR1442600).

Disclosure of conflict of interest

None.

Address correspondence to: Drs. Liang Duan and Gening Jiang, Department of Thoracic Surgery, Shanghai Pulmonary Hospital, Tongji University School of Medicine, Shanghai, P. R. China. E-mail: duan-liang@163.com (LD); jgnwp@aliyun.com (GNJ); Dr. Xue Zhang, Department of Dermatology, Xinhua Hospital, Shanghai Jiao Tong University School of Medicine, Shanghai, P. R. China. E-mail: zhangxue0101@hotmail.com (XZ)

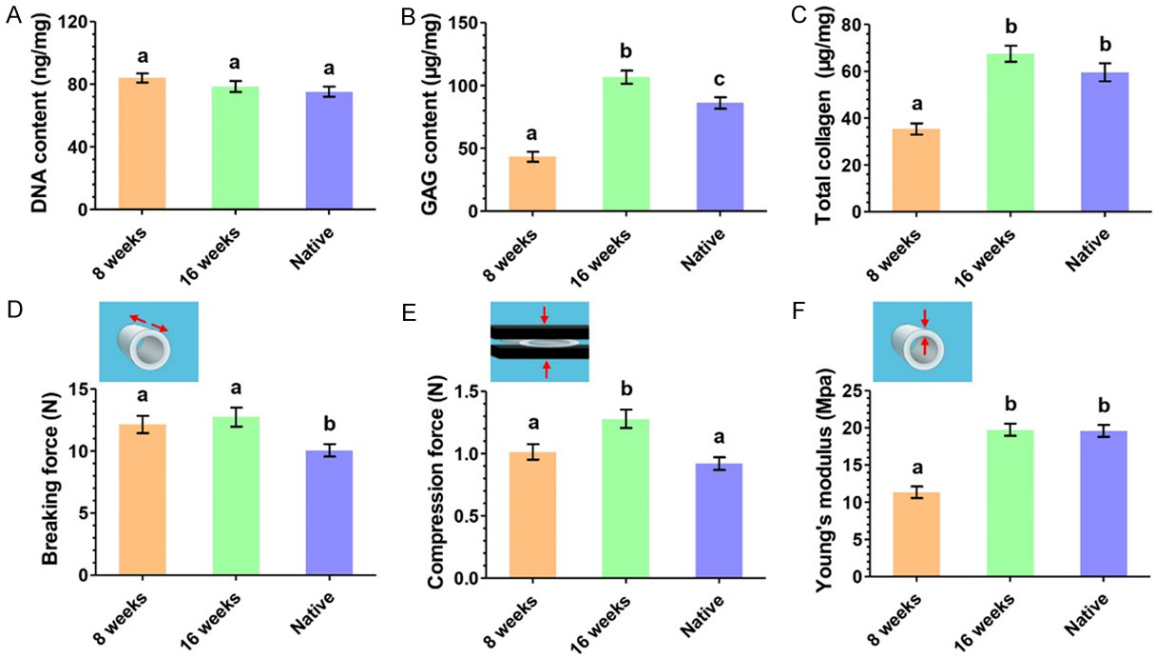

Figure 9. Quantitative evaluations of the neocartilage *in vivo*. DNA content (A), GAG content (B), total collagen (C), breaking force (D), compression force (E), and Young's modulus (F) of the neocartilage increase with extended *in vivo* culture time. These are higher than those of the fresh native trachea group (native) after 16 weeks of *in vivo* culture. Letters in lowercase indicate significant differences among the groups ($P<0.05$). The red arrows indicate the direction of the force.

References

[1] Bae SW, Lee KW, Park JH, Lee J, Jung CR, Yu J, Kim HY and Kim DH. 3D bioprinted artificial trachea with epithelial cells and chondrogenic-differentiated bone marrow-derived mesenchymal stem cells. Int J Mol Sci 2018; 19: 16-24.

[2] Lee JY, Park JH and Cho DW. Comparison of tracheal reconstruction with allograft, fresh xenograft and artificial trachea scaffold in a rabbit model. J Artif Organs 2018; 21: 325-331.

[3] Taniguchi D, Matsumoto K, Tsuchiya T, Machino R, Takeoka Y, Elgalad A, Gunge K, Takagi K, Taura Y, Hatachi G, Matsuo N, Yamasaki N, Nakayama K and Nagayasu T. Scaffold-free trachea regeneration by tissue engineering with bio-3D printing. Interact Cardiovasc Thorac Surg 2018; 26: 745-752.

[4] Best CA, Pepper VK, Ohst D, Bodnyk K, Heuer E, Onwuka EA, King N, Strouse R, Grischkan J, Breuer CK, Johnson J and Chiang T. Designing a tissue-engineered tracheal scaffold for preclinical evaluation. Int J Pediatr Otorhinolaryngol 2018; 104: 155-160.

[5] Hong P, Bezuhly M, Graham ME and Gratzer PF. Efficient decellularization of rabbit trachea to generate a tissue engineering scaffold biomatrix. Int J Pediatr Otorhinolaryngol 2018; 112: 67-74.

[6] Rosli NA, Ahmad I, Anuar FH and Abdullah I. Application of polymethylmethacrylate-grafted cellulose as reinforcement for compatibilised polylactic acid/natural rubber blends. Carbohydr Polym 2019; 213: 50-58.

[7] Chen J, Yuan Z, Liu Y, Zheng R, Dai Y, Tao R, Xia H, Liu H, Zhang Z, Zhang W, Liu W, Cao Y and Zhou G. Improvement of in vitro three-dimensional cartilage regeneration by a novel hydrostatic pressure bioreactor. Stem Cells Transl Med 2017; 6: 982-991.

[8] Xue J, Feng B, Zheng R, Lu Y, Zhou G, Liu W, Cao Y, Zhang Y and Zhang WJ. Engineering ear-shaped cartilage using electrospun fibrous membranes of gelatin/polycaprolactone. Biomaterials 2013; 34: 2624-2631.

[9] Zang M, Zhang Q, Chang EI, Mathur AB and Yu P. Decellularized tracheal matrix scaffold for tracheal tissue engineering: in vivo host response. Plast Reconstr Surg 2013; 132: 549e-559e.

[10] Batioglu-Karaaltin A, Ovali E, Karaaltin MV, Yener M, Yilmaz M, Eyupoglu F, Yilmaz YZ, Bozkurt ER, Demir N, Konuk E, Bozdag ES, Yigit O and Cansiz H. Decellularization of trachea with combined techniques for tissue-engineered trachea transplantation. Clin Exp Otorhinolaryngol 2019; 12: 86-94.

[11] Haykal S, Zhou Y, Marcus P, Salna M, Machuca T, Hofer SO and Waddell TK. The effect of de-

cellularization of tracheal allografts on leukocyte infiltration and of recellularization on regulatory T cell recruitment. Biomaterials 2013; 34: 5821-5832.
[12] Gong YY, Xue JX, Zhang WJ, Zhou GD, Liu W and Cao Y. A sandwich model for engineering cartilage with acellular cartilage sheets and chondrocytes. Biomaterials 2011; 32: 2265-2273.
[13] Xu Y, Li D, Yin Z, He A, Lin M, Jiang G, Song X, Hu X, Liu Y, Wang J, Wang X, Duan L and Zhou G. Tissue-engineered trachea regeneration using decellularized trachea matrix treated with laser micropore technique. Acta Biomater 2017; 58: 113-121.
[14] Zhang Y, Xu Y, Liu Y, Dan L, Yin Z, Huo Y, Jiang G, Yang Y, Wang Z, Li Y, Lu F, Liu Y, Duan L and Zhou G. Porous decellularized trachea scaffold prepared by a laser micropore technique. J Mech Behav Biomed Mater 2019; 90: 96-103.
[15] Lutolf MP and Hubbell JA. Synthetic biomaterials as instructive extracellular microenvironments for morphogenesis in tissue engineering. Nat Biotechnol 2005; 23: 47-55.
[16] Cha MH, Do SH, Park GR, Du P, Han KC, Han DK and Park K. Induction of re-differentiation of passaged rat chondrocytes using a naturally obtained extracellular matrix microenvironment. Tissue Eng Part A 2013; 19: 978-988.
[17] Wu YN, Yang Z, Hui JH, Ouyang HW and Lee EH. Cartilaginous ECM component-modification of the micro-bead culture system for chondrogenic differentiation of mesenchymal stem cells. Biomaterials 2007; 28: 4056-4067.
[18] Voss A, McCarthy MB, Hoberman A, Cote MP, Imhoff AB, Mazzocca AD and Beitzel K. Extracellular matrix of current biological scaffolds promotes the differentiation potential of mesenchymal stem cells. Arthroscopy 2016; 32: 2381-2392, e2381.
[19] He X, Feng B, Huang C, Wang H, Ge Y, Hu R, Yin M, Xu Z, Wang W, Fu W and Zheng J. Electrospun gelatin/polycaprolactone nanofibrous membranes combined with a coculture of bone marrow stromal cells and chondrocytes for cartilage engineering. Int J Nanomedicine 2015; 10: 2089-2099.
[20] Homicz MR, Schumacher BL, Sah RL and Watson D. Effects of serial expansion of septal chondrocytes on tissue-engineered neocartilage composition. Otolaryngol Head Neck Surg 2002; 127: 398-408.
[21] Jia S, Zhang T, Xiong Z, Pan W, Liu J and Sun W. In vivo evaluation of a novel oriented scaffold-bmsc construct for enhancing full-thickness articular cartilage repair in a rabbit model. PLoS One 2015; 10: e0145667.
[22] Zhou G, Liu W, Cui L, Wang X, Liu T and Cao Y. Repair of porcine articular osteochondral defects in non-weightbearing areas with autologous bone marrow stromal cells. Tissue Eng 2006; 12: 3209-3221.
[23] Wang Y, Kim UJ, Blasioli DJ, Kim HJ and Kaplan DL. In vitro cartilage tissue engineering with 3D porous aqueous-derived silk scaffolds and mesenchymal stem cells. Biomaterials 2005; 26: 7082-7094.
[24] Pittenger MF, Mackay AM, Beck SC, Jaiswal RK, Douglas R, Mosca JD, Moorman MA, Simonetti DW, Craig S and Marshak DR. Multilineage potential of adult human mesenchymal stem cells. Science 1999; 284: 143-147.
[25] Li D, Zhu L, Liu Y, Yin Z, Liu Y, Liu F, He A, Feng S, Zhang Y, Zhang Z, Zhang W, Liu W, Cao Y and Zhou G. Stable subcutaneous cartilage regeneration of bone marrow stromal cells directed by chondrocyte sheet. Acta Biomater 2017; 54: 321-332.
[26] Moran JM, Pazzano D and Bonassar LJ. Characterization of polylactic acid-polyglycolic acid composites for cartilage tissue engineering. Tissue Eng 2003; 9: 63-70.
[27] Yuan Z, Liu S, Hao C, Guo W, Gao S, Wang M, Chen M, Sun Z, Xu Y, Wang Y, Peng J, Yuan M and Guo QY. AMECM/DCB scaffold prompts successful total meniscus reconstruction in a rabbit total meniscectomy model. Biomaterials 2016; 111: 13-26.
[28] Yan D, Zhou G, Zhou X, Liu W, Zhang WJ, Luo X, Zhang L, Jiang T, Cui L and Cao Y. The impact of low levels of collagen IX and pyridinoline on the mechanical properties of in vitro engineered cartilage. Biomaterials 2009; 30: 814-821.
[29] Reddy GK and Enwemeka CS. A simplified method for the analysis of hydroxyproline in biological tissues. Clin Biochem 1996; 29: 225-229.
[30] Birchall M and Macchiarini P. Airway transplantation: a debate worth having? Transplantation 2008; 85: 1075-1080.
[31] Sakaguchi Y, Sato T, Muranishi Y, Yutaka Y, Komatsu T, Omori K, Nakamura T and Date H. Development of a novel tissue-engineered nitinol frame artificial trachea with native-like physical characteristics. J Thorac Cardiovasc Surg 2018; 156: 1264-1272.
[32] Gilevich IV, Sotnichenko AS, Karal-Ogly DD, Gubareva EA, Kuevda EV, Polyakov IS, Lapin BA, Orlov SV, Porkhanov VA and Chekhonin VP. In vivo experimental study of biological compatibility of tissue engineered tracheal construct in laboratory primates. Bull Exp Biol Med 2018; 164: 770-774.
[33] Pei M, Li JT, Shoukry M and Zhang Y. A review of decellularized stem cell matrix: a novel cell expansion system for cartilage tissue engi-

neering. Eur Cell Mater 2011; 22: 333-343; discussion 343.
[34] Kojima K and Vacanti CA. Tissue engineering in the trachea. Anat Rec (Hoboken) 2014; 297: 44-50.
[35] Tanaka H, Maeda K and Okita Y. Transplantation of the cryopreserved tracheal allograft in growing rabbits. J Pediatr Surg 2003; 38: 1707-1711.
[36] Conconi MT, De Coppi P, Di Liddo R, Vigolo S, Zanon GF, Parnigotto PP and Nussdorfer GG. Tracheal matrices, obtained by a detergent-enzymatic method, support in vitro the adhesion of chondrocytes and tracheal epithelial cells. Transpl Int 2005; 18: 727-734.
[37] Pelttari K, Steck E and Richter W. The use of mesenchymal stem cells for chondrogenesis. Injury 2008; 39 Suppl 1: S58-65.
[38] Csaki C, Schneider PR and Shakibaei M. Mesenchymal stem cells as a potential pool for cartilage tissue engineering. Ann Anat 2008; 190: 395-412.
[39] Cancedda R, Dozin B, Giannoni P and Quarto R. Tissue engineering and cell therapy of cartilage and bone. Matrix Biol 2003; 22: 81-91.
[40] Pieper JS, van der Kraan PM, Hafmans T, Kamp J, Buma P, van Susante JL, van den Berg WB, Veerkamp JH and van Kuppevelt TH. Crosslinked type II collagen matrices: preparation, characterization, and potential for cartilage engineering. Biomaterials 2002; 23: 3183-3192.
[41] Young RD, Vaughan-Thomas A, Wardale RJ and Duance VC. Type II collagen deposition in cruciate ligament precedes osteoarthritis in the guinea pig knee. Osteoarthritis Cartilage 2002; 10: 420-428.
[42] Tavassoli A, Matin MM, Niaki MA, Mahdavi-Shahri N and Shahabipour F. Mesenchymal stem cells can survive on the extracellular matrix-derived decellularized bovine articular cartilage scaffold. Iran J Basic Med Sci 2015; 18: 1221-1227.
[43] Chen YC, Chen RN, Jhan HJ, Liu DZ, Ho HO, Mao Y, Kohn J and Sheu MT. Development and characterization of acellular extracellular matrix scaffolds from porcine menisci for use in cartilage tissue engineering. Tissue Eng Part C Methods 2015; 21: 971-986.